Multi-Objective Optimization Using Kriging Model and Data Mining

Shinkyu Jeong* and Shigeru Obayashi**
Institute of Fluid Science
Tohoku University, Katahira 2-1-1 Sendai, Japan 980-8577

Abstract

In this study, a surrogate model is applied to multi-objective aerodynamic optimization design. For the balanced exploration and exploitation, each objective function is converted into the Expected Improvement (EI) and this value is used as fitness value in the multi-objective optimization instead of the objective function itself. Among the non-dominated solutions about EIs, additional sample points for the update of the Kriging model are selected. The present method was applied to a transonic airfoil design. Design results showed the validity of the present method. In order to obtain the information about design space, two data mining techniques are applied to design results: Analysis of Variance (ANOVA) and the Self-Organizing Map (SOM).

Key Word : Kriging Model, Expected Improvement, Multi-Objective Optimization, Data Mining, Analysis of Variance (ANOVA), Self-Organizing Map (SOM)

Nomenclature

c_i	best-matching unit	β	constant global model of Kriging model
$E[I(\cdot)]$	expected improvement	$\hat{\beta}$	estimated value of constant global model
$\boldsymbol{r}'$	vector of correlation values for Kriging model	ϕ	standard normal density
$\boldsymbol{R}$	correlation matrix for Kriging model	Φ	standard normal distribution
$s(\cdot)$	root mean square error of the predictor	$\hat{\mu}_{total}$	total mean of model
t/c	ratio of airfoil thickness to chord length	$\boldsymbol{\theta}$	vector of correlation parameters for Kriging model
$\mathbf{x}$	vector denoting position in the design space	θ_k	k_{th} element of $\boldsymbol{\theta}$
x	scalar component of $\mathbf{x}$	$\hat{\sigma^2}$	estimated variance of Kriging model
$\hat{y}(\cdot)$	estimated function value	$\hat{\sigma}_{total}^2$	total variance of model
$\boldsymbol{y}$	vector of response data	$\boldsymbol{w_i}$	weight vector of self-organizing map
$Z(\cdot)$	deviation from the global model		

* Research Associate
E-mail : jeong@edge.ifs.tohoku.ac.jp Tel : 022-217-5724 Fax : 022-217-5724
** Professor

Introduction

Recently, surrogate models[1] are widely used in the field of engineering design to ease the computational burden of optimization. However, most of surrogate models have a problem of its fidelity because the function value predicted by surrogate models contains an uncertainty in it. Especially, in the aerodynamic design field[2,3] where the response functions are often nonlinear and multimodal, surrogate models cannot provide the sufficient fidelity for the optimization design.

In order to make up for the low fidelity of surrogate model, Jones et al. suggested the efficient global optimization (EGO) algorithm[4]. It makes use of the Kriging model, which is developed in the field of spatial statistics and geostatics, as a surrogate model. The Kriging model predicts not the function value itself but the distribution of the function value. Using the distribution of the function value, one can predict not only the function value but also its uncertainty. The uncertainty information plays a key role in EGO. In EGO, the exploration is based on the potential of being superior to the current optimum instead of the objective function value. According to the concept of EGO, the solution that has a high predicted function value with a large error may be a more promising than the solution that has a low predicted function value with a small error in the minimization problem. EGO makes it possible to realize the balanced exploitation and exploration. EGO was successfully applied to the single objective aerodynamic optimization design[5].

In this study, EGO is extended to multi-objective aerodynamic design problem. For the multi-objective problem, Knowles et al. suggested ParEGO (Pareto EGO) which converts multiple objective functions into a single objective function by using a parameterized weighting vector[6]. Although ParEGO showed a good performance on several test functions, its ability to find the Pareto front largely depends on the selection of the weighting vector. Thus, in this study, each objective function is converted into the EI of objective function and this value is used as the fitness value in the multi-objective optimization. This makes it possible to obtain the non-dominated solutions about EIs without using the weight vectors. From these non-dominated solutions, designer can select the additional sample points for the update of the Kriging model. This method prevents from an incorrect exploration of Pareto front, which may be caused by the weighting vector.

In the multi-objective optimization, a correct non-dominated solutions exploration is very important. However, in the field of engineering design, it is also important to determine the final design from nominated solutions, such as non-dominated solutions of multi-objective problem. Thus, it is preferable for a designer to supply the non-dominated solutions with some useful information for the final design decision. Information about the design space, such as trade-off relations between objective functions and the relations between design variables and objective functions, will be one of the useful information for the decision of final design. Furthermore, this information makes it possible to simplify the design problem by eliminating the design variables that do not have a significant influence on the objective functions.

The process to find the information from the design results is called 'data mining'. In this study, advanced data mining techniques, Analysis of Variance (ANOVA) and Self-Organizing Map (SOM), are introduced. The former uses the variance of the objective function due to design variables on surrogate models. ANOVA can identify not only the effect of each design variable but also the effect of interactions between design variables on objective functions. ANOVA expresses the information in a quantitative way. On the other hand, SOM employs a nonlinear projection algorithm from high to low dimension and a clustering technique. This method can visualize not only the relation between design variables and objective functions but also the trade-off between objective functions. The method expressed the information in a qualitative way.

EGO for Multi-Objective Problem: EGOMOP

Kriging Model

The present Kriging model is composed of a constant global model β and the Gaussian stochastic process $Z(\mathbf{x})$ representing a deviation from the global model:

$$y(\mathbf{x}) = \beta + Z(\mathbf{x}) \tag{1}$$

where $\mathbf{x}$ is an m-dimensional vector (m design variables). The correlation between $Z(\mathbf{x}^i)$ and $Z(\mathbf{x}^j)$ is strongly related to the distance between the two corresponding points, $\mathbf{x}^i$ and $\mathbf{x}^j$. In the Kriging model, a specially weighted distance is used instead of the Euclidean distance because the latter weighs all design variables equally. The distance function between the point at $\mathbf{x}^i$ and $\mathbf{x}^j$ is expressed as:

$$d(\mathbf{x}^i, \mathbf{x}^j) = \sum_{k=1}^{m} \theta_k |x_k^i - x_k^j| \tag{2}$$

where $\Theta_k (0 \le \Theta_k \le \infty)$ is the k_{th} element of the correlation vector parameter Θ. The correlation between the points, $\mathbf{x}^i$ and $\mathbf{x}^j$, is defined as:

$$Corr[Z(\mathbf{x}^i), Z(\mathbf{x}^j)] = \exp[-d(\mathbf{x}^i, \mathbf{x}^j)] \tag{3}$$

The Kriging predictor [7] is

$$\hat{y}(\mathbf{x}) = \hat{\beta} + \mathbf{r}' \mathbf{R}^{-1} (\mathbf{y} - \mathbf{1}\hat{\beta}) \tag{4}$$

where $\hat{\beta}$ is the estimated value of β and can be calculated using the following equation:

$$\hat{\beta} = \frac{\mathbf{1}' \boldsymbol{R}^{-1} \boldsymbol{y}}{\mathbf{1}' \boldsymbol{R}^{-1} \mathbf{1}} \tag{5}$$

$\mathbf{R}$ denotes the $n \times n$ matrix whose (i, j) entry is $Corr[Z(\mathbf{x}^i), Z(\mathbf{x}^j)]$ and $\mathbf{1}$ denotes an n-dimensional unit vector. $\mathbf{r}$ is the vector whose i_{th} element is

$$r_i(\mathbf{x}) = Corr[Z(\mathbf{x}), Z(\mathbf{x}^i)] \tag{6}$$

and $\mathbf{y} = [y(\mathbf{x}^1), \cdots\cdots, y(\mathbf{x}^n)]$.

The unknown parameter, Θ, for the Kriging model can be estimated by maximizing the following likelihood function:

$$Ln(\hat{\beta}, \hat{\sigma^2}, \boldsymbol{\theta}) = -\frac{n}{2} ln(\hat{\sigma^2}) - \frac{1}{2} ln(|\mathbf{R}|) \tag{7}$$

where $\hat{\sigma^2}$ can be calculated as follows:

$$\hat{\sigma^2} = \frac{(\boldsymbol{y} - \mathbf{1}\hat{\beta})' \boldsymbol{R} (\boldsymbol{y} - \mathbf{1}\hat{\beta})}{n} \tag{8}$$

Maximizing the likelihood function is an m-dimensional unconstrained non-linear optimization problem. In this paper, a simple genetic algorithm is adopted to solve this problem. This problem requires several thousands of matrix inversion which consumes a lot of computational time. However, compared with computational time of high-fidelity evaluation of the objective function, its computational time is negligible.

The accuracy of the predicted value depends largely on the distance from the sample

points. Intuitively, the closer point $\mathbf{x}$ is to the sample points, the more accurate the prediction, $\hat{y}(\mathbf{x})$, becomes. This is expressed in the following equation:

$$s^2(\mathbf{x}) = \hat{\sigma}^2\left[1 - \mathbf{r}'\mathbf{R}^{-1}\mathbf{r} + \frac{1 - \mathbf{1}\mathbf{R}^{-1}\mathbf{r}}{\mathbf{1}'\mathbf{R}^{-1}\mathbf{1}}\right] \tag{9}$$

where $s^2(\mathbf{x})$ is the mean square error at point $\mathbf{x}$, indicating the uncertainty of the estimated value.

Expected Improvement

Expected Improvement (EI) means the potential of being superior to than current optimum. EI considers the predicted function value and its uncertainty at the same time. Thus, in the minimization problem, the solution with large objective function value and large uncertainty may be smaller than the solution with small objective function and small uncertainty. This feature makes it possible to explore the design space globally. EI [8] in the minimization problem is expressed as following:

$$\begin{aligned} E[I(\mathbf{x})] &= E\left[\max(f_{\min} - \hat{y}, 0)\right] \\ &= (f_{\min} - \hat{y})\Phi\left(\frac{f_{\min} - \hat{y}}{s}\right) + s\phi\left(\frac{f_{\min} - \hat{y}}{s}\right) \end{aligned} \tag{10}$$

where Φ and ϕ are the standard distribution and normal density, respectively.

In this study, EI of objective function is directly used as fitness values in the multi-objective optimization. Multi-objective genetic algorithm (MOGA) maximizes EIs of objective functions to finds the non-dominated solutions about EIs and several points are selected from the non-dominated solutions to update the Kriging model. Overall procedure of EGOMOP is shown in Fig. 1.

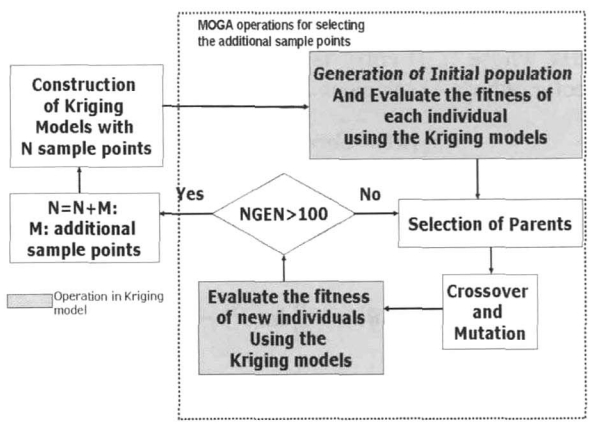

Fig. 1. Overall procedure of EGOMOP used in this study

Data Mining

Analysis of Variance (ANOVA)

ANOVA is one of the data mining techniques showing the effect of each design variable on the objective functions in a quantitative way. ANOVA uses the variance of the functions due to

the design variables on surrogate models. By decomposing the total variance of the function into the variance component due to each design variable, the influence of each design variable on the objective function can be calculated. Decomposition is accomplished by integrating variables out of the function $\hat{y}$. The total mean ($\hat{\mu}_{total}$) and the variance ($\hat{\sigma}^2_{total}$) of the function $\hat{y}$ are as follows:

$$\hat{\mu}_{total} = \int \cdots \int \hat{y}(x_1, \cdots\cdots, x_m) dx_1, \cdots, dx_m \tag{11}$$

$$\hat{\sigma}^2_{total} = \int \cdots \int \left[\hat{y}(x_1, \cdots\cdots, x_m) - \hat{\mu}_{total}\right]^2 dx_1, \cdots, dx_m \tag{12}$$

The main effect of variable x_i is

$$\hat{\mu}_i = \int \cdots \int \hat{y}(x_1, \cdots, x_m) dx_1, \cdots, dx_{i-1} dx_{i+1}, \cdots, dx_m - \hat{\mu}_{total} \tag{13}$$

The variance due to the design variable x_i is given as:

$$\hat{\sigma}^2_i = \int \left[\hat{\mu}_i(x_i)\right]^2 dx_i \tag{14}$$

The proportion of the variance due to design variable x_i to total variance of the function can be expressed by dividing Eq. (14) by Eq. (12).

$$\frac{\hat{\sigma}^2_i}{\hat{\sigma}^2_{total}} = \frac{\int \left[\hat{\mu}_i(x_i)\right]^2 dx_i}{\int \left[\hat{y}(x_1, \cdots\cdots, x_m) - \hat{\mu}_{total}\right]^2 dx_1, \cdots, dx_m} \tag{15}$$

This value indicates the effect of design variable x_i on the objective function $\hat{y}$.

Self-Organizing Map (SOM)

SOM is one of the unsupervised neural networks techniques that classify, organize, and visualize large data sets. SOM is a nonlinear projection algorithm[9] from high- to low-dimensional space. This projection is based on self-organization of a low-dimensional array of neurons. In the projection algorithm, the weights between the input vector and the array of neurons are adjusted to represent features of the high-dimensional data on the low-dimensional map. The closer two patterns are in the original space, the closer the response of two neighboring neurons in the low-dimensional space. Thus, SOM reduces the dimension of input data while preserving their features. While ANOVA shows the relation between the design variables and the objective function quantitatively, SOM shows it qualitatively.

A neuron used in SOM is associated with weight vector $\mathbf{w}_i = [w_{i1}, w_{i2}, \cdots, w_{im}]$ (i=1,$\cdots$, N), where m is the dimension of the input vector $\mathbf{x}$ and N is the number of neurons. Each neuron is connected to its adjacent neurons by a neighborhood relation. In this study, the Batch-SOM algorithm is used for the training of SOM. The algorithm consists of two steps that are iterated until no more significant changes occur: search of the best-matching unit (BMU) c_i for all input data $\{\mathbf{x}_i\}$ and update of weight vector $\{\mathbf{w}_i\}$ near the best-matching unit. The Batch-SOM algorithm can be formulated as follows:

$$c_i = \arg\min \|\mathbf{x}_i - \mathbf{w}_j\| \tag{16}$$

$$\mathbf{w}^*_j = \frac{\sum_i h_{jc_i} \mathbf{x}_i}{\sum_i h_{jc_i}} \tag{17}$$

where $\mathbf{w}^*_j$ is the updated weight vector. The neighborhood relationship between neuron j and the best-matching unit c_i is defined by the following Gaussian-like function:

$$h_{jc_i} = \exp\left(\frac{d_{jc_i}^2}{r_t^2}\right) \tag{18}$$

where d_{jc_i} denotes the Euclidean distance between the neuron k and the best-matching unit c_i on the map, and r_t denotes the neighborhood radius, which is decreased with the iteration steps t. Compared with the standard SOM, which updates the weight vector when each record is read and matched, the Batch-SOM takes a 'batch' of data (typically all records), and performs a 'collected' update of the weight vectors after all records have been matched. This is much like 'epoch' learning in supervised neural networks. The Batch-SOM is a more robust approach, since it mediates over a large number of learning steps. The uniqueness of the map is ensured by adoption of Batch-SOM and the linear initialization for input data.

In this study, commercial software Viscovery® SOMine[10] produced by Eudaptics GmbH is used. Much like other SOM, SOMine creates a map in a two-dimensional hexagonal grid. Starting from numerical, multivariate data, the neurons on the grid gradually adapt to the intrinsic shape of the data distribution. As the position on the grid reflects the neighborhood within the data, features of the data distribution can be read from the emerging map on the grid. The trained SOM is systematically converted into visual information. Once the high-dimensional data is projected onto the two-dimensional regular grid, the map can be used for visualization and data mining. It is efficient to group all neurons by the similarity to facilitate SOM for qualitative analysis, because number of neurons on the SOM is large as a whole. This process of grouping is called 'clustering'. Hierarchical agglomerative algorithm is used for the clustering here. First, each node itself forms a single cluster, and two clusters, which are adjacent in the map, are merged in each step. The distance between two clusters is calculated by using the SOM-ward distance [10]. The number of clusters is determined by the hierarchical sequence of clustering. A relatively small number of clusters are used for visualization, while a large number of clusters are used for the generation of weight vectors for respective design variables.

Application to Aerodynamic Design

Definition of Optimization Problem

The present method is applied to a transonic airfoil design. In the transonic region, the flowfield is drastically changed even with a small fluctuation. For the robust transonic airfoil design, the objective functions are defined as follows:

Minimize *obj1*: Drag at fixed lift of 0.75 (Mach=0.70)
obj2: Drag at fixed lift of 0.67 (Mach=0.74)

subject to $t/c > 11\%$

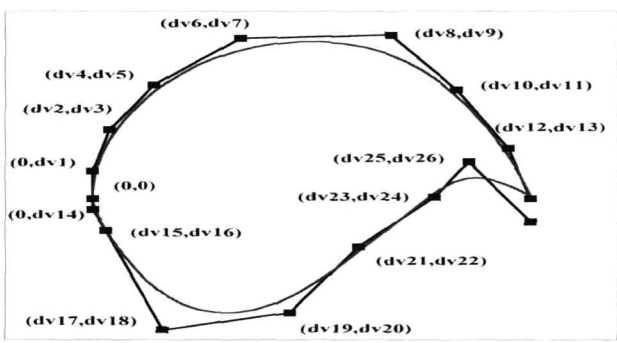

Fig. 2. Airfoil geometry definition using NURBS

First objective function is for the design condition (at low speed) and the other is for the off-design condition (at high speed). The design constraint is the maximum thickness of the airfoil.

The geometry of the airfoil is defined using Non-Uniform Rational B-Spline (NURBS) [11] to represent free-form shape. A total of 26 design variables are used to represent shape of the airfoil exactly as shown in Fig. 2. The search region of each design variable is determined to avoid unrealistic airfoil geometry such as a fish-tailed airfoil.

Construction of Kriging Model

Initial sample points of the Kriging model are selected using Latin Hypercube Sampling (LHS)[12] with the constraint evaluation. Once LHS selects a point (airfoil), the point is checked whether it satisfies the design constraint or not. If the point satisfies the constraint, the point is selected as sample point, if not, the point is rejected. A total of 26 sample points are selected with 50 divisions in LHS. Design variable distribution of 26 sample points are shown in Fig. 3. Sample points are uniformly spread in the search region of all design variables except dv7. This means that the airfoil with a small value of dv7 cannot satisfy design constraint.

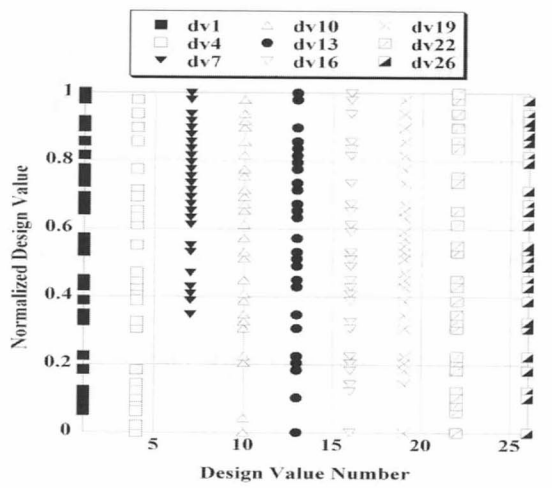

Fig. 3. Distribution of initial sample points in search region

In case of LHS without the constraint evaluation, only 13 points satisfy the design constraint with the same number of divisions. It means that 37 sample points are located in the infeasible design space. By using LHS coupled with the constraint evaluation, it is possible to select the sample points only from the feasible design space.

Drag performances of 26 sample airfoils are evaluated using a Navier-Stokes calculation. With the data obtained from the Navier-Stokes analysis, the Kriging parameter θ is determined by solving maximization problem of Eq. (7).

Design Results

In the Kriging models, EIs of two objective functions are maximized by using MOGA to find the non-dominated solutions about EIs. In the present MOGA, number of populations and generations are 512 and 100, respectively. Fig. 4 shows the non-dominated solutions about EIs after the first EGOMOP loop. EIs of objective functions are in the trade-off relation.

Among these non-dominated solutions, three points are selected for the update of the Kriging

models: i) the point whose EI of *obj1* is the largest, ii) the point whose EI of *obj2* is the largest, iii) mid point in the non-dominated solutions.

Fig. 5 shows the non-dominated solutions about EIs obtained after the several EGOMOP loops. The values of EI are gradually decreased as EGOMOP loop iterated. It means that the accuracy near the Pareto front is improved by adding the additional sample points.

Fig. 6 shows the initial sample points and the additional points selected by using EGOMOP. Total 89 points are selected in this design. The additional points selected by EGOMOP show better performances than the initial sample points. It means that EGOMOP algorithm correctly selected the additional points for update of the Kriging models.

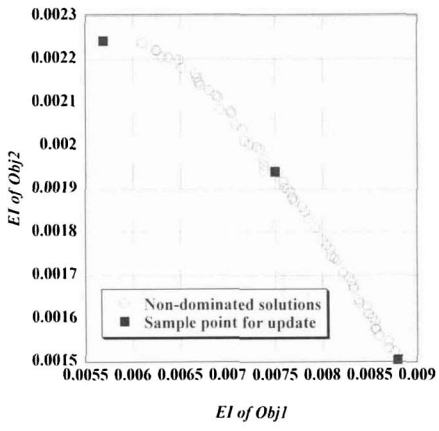

Fig. 4. Non-dominated solutions about EI

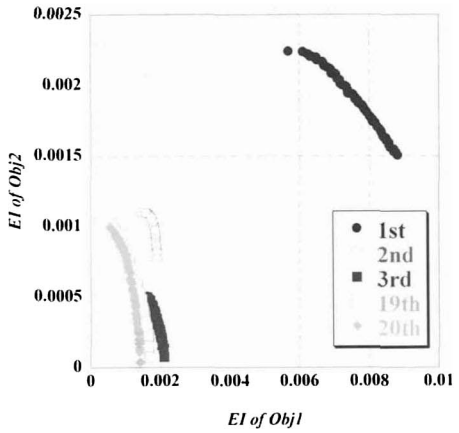

Fig. 5. Non-dominated solutions of EIs

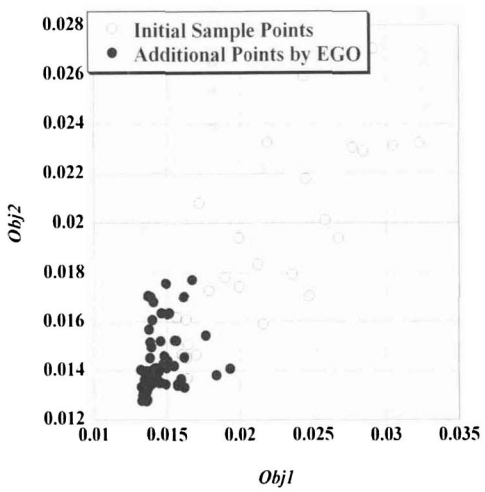

Fig. 6. Initial sample points and additional points selected by EGO

The geometry and the pressure distributions of designed airfoil, which shows the best performances about both objective functions among 89 sample points, are compared with those of RAE2822 airfoil. The designed airfoil maintains shock-free condition at both flow cases, while RAE2822 represents strong shocks on upper surface. Drag performance of both airfoils are also compared in Table 1.

Table 1. Comparison of drag performances between RAE2822 and designed airfoil

	Obj1	Obj2
RAE2822	0.0135	0.01582
Design	0.0132	0.0127

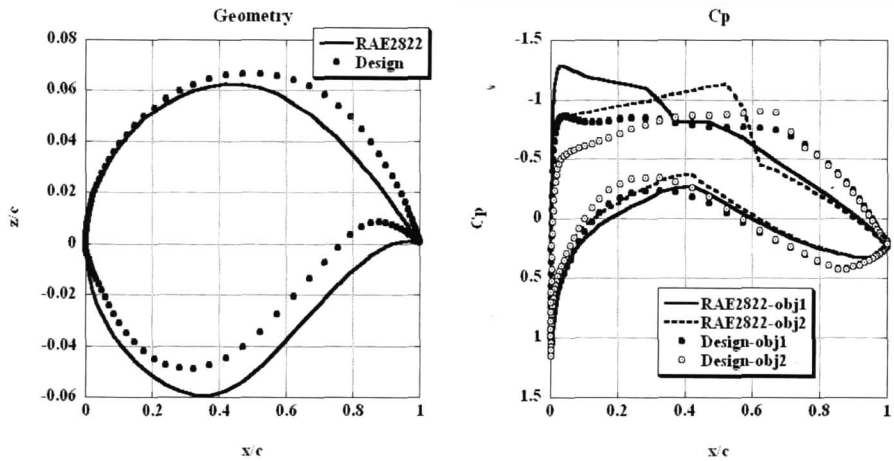

Fig. 7. Comparison of geometry and pressure distributions between RAE2822 and designed airfoil

Result of Data Mining

ANOVA

Total variances of objective functions were decomposed into the variance due to each design variable. The variance of design variables and the interactions in which the proportion to the total variable is larger than 1.0% are shown in Fig. 8. According to Fig. 8, dv3 gives the largest effect on *obj1* and dv9 gives the largest effect on *obj2*. dv7 and dv3-dv7, dv3-dv9 and dv7-dv9 give much effect on objective functions.

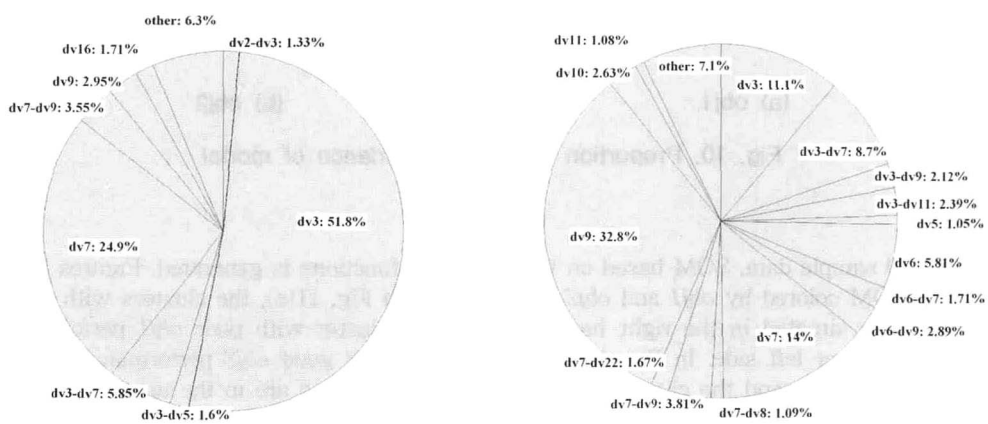

(a) obj1 (b) obj2

Fig. 8. Proportion to the total variance of model

However, it is difficult to understand the relation between aerodynamic performance and airfoil geometry intuitively because design variables defined by NURBS are not for the data mining but for the detailed expression of airfoil geometry. Thus, design variables defined by NURBS are transformed into the design variables which are more familiar to aerodynamic engineers such as the leading edge radius and the maximum thickness position. The transformed design variables are shown in Fig. 9.

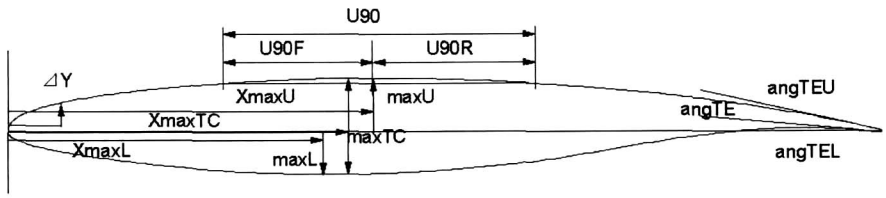

Fig. 9. Transformed design variables

With these design variables, ANOVA is performed again. The results are shown in Fig. 10. According to Fig. 10, ΔY gives the largest effect on *obj1* and XmaxU gives the largest effect on *obj2*. These findings correspond to general aerodynamic knowledge that the leading-edge radius (ΔY) and the maximum thickness position (XmaxU) are strongly related to low and high speed performance, respectively.

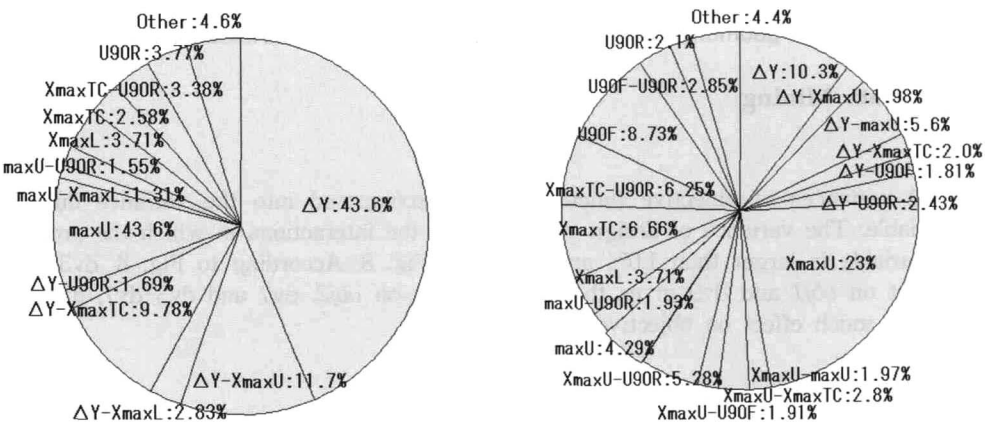

(a) obj1 **(b) obj2**

Fig. 10. Proportion to the total variance of model

SOM

With 89 sample data, SOM based on two objective functions is generated. Figures 11(a) and 11(b) show SOM colored by *obj1* and *obj2*, respectively. In Fig. 11(a), the clusters with good *obj1* performance are situated in the right-hand side and the cluster with poor *obj1* performance are located in the upper left side. In Fig. 11(b), the clusters with good *obj2* performance are located in the right-hand side and the cluster with poor *obj2* performance are in the upper and the lower corner of left-hand side. Figures 12 (a) and 12 (b) show SOM colored by dv3 and dv9 which gives the largest effect on the *obj1* and the *obj2*, respectively, according to the ANOVA. In Fig. 12 (a), the clusters with large dv3 values are located in the upper left corner. In Fig. 11(a), these clusters also have poor *obj1* performance. This means that large dv3 values are associated with poor *obj1* performance. In Fig. 12 (b), the clusters with small dv9 values are located in left-hand

side and the clusters with large dv9 values are in the right-hand side. Its color patterns are opposite to those of Fig. 11 (b). This means that small dv9 values are related to poor *obj2* performance vice versa. The visualization results of SOM agree with the results of ANOVA.

SOM is also colored by the transformed design variables. Figures 13 (a) and 13 (b) show SOM colored by ΔY and XmaxU. In Fig. 13 (a), the clusters with large ΔY values are located in the upper left side. The distribution of color is similar to that of SOM colored by *obj1*. This means that large ΔY values are related to poor *obj1* performance. In Fig. 13 (b), the clusters with small XmaxU values are situated in the upper and the lower corner of left hand side. Its color patterns are opposite to those of Fig. 11 (b). This means that small XmaxU values are associated with poor *obj2* performance vice versa. These results also coincide with those of ANOVA.

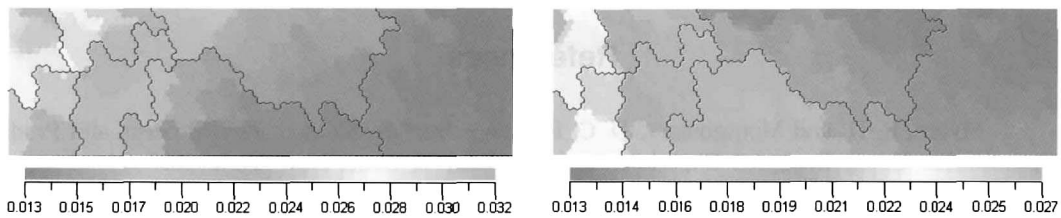

(a) SOM colored by obj1 (b) SOM colored by obj2

Fig. 11. SOM colored by objective functions

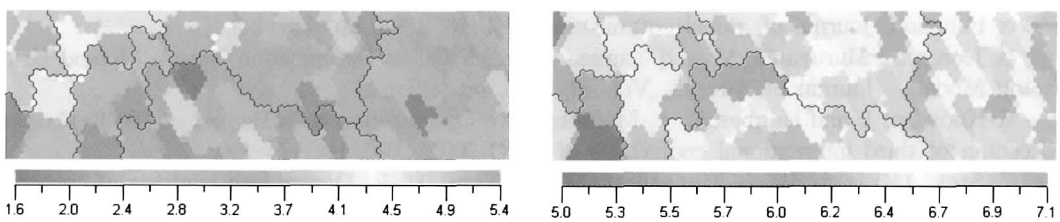

(a) SOM colored by dv3 (b) SOM colored by dv9

Fig. 12. SOM colored by selected design variables

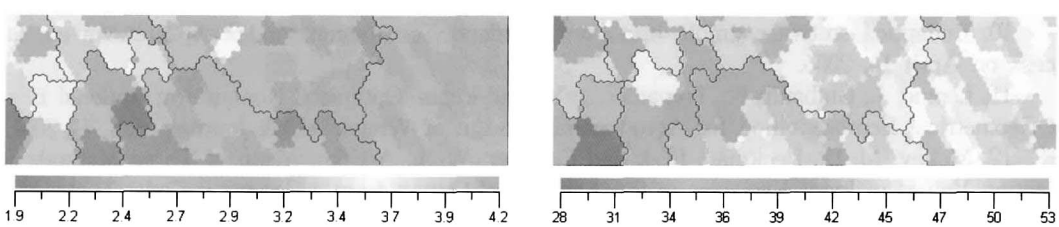

(a) SOM colored by ΔY (b) SOM colored by XmaxU

Fig. 13. SOM colored by selected design variables

Conclusion

In this study, a surrogate model was applied to multi-objective aerodynamic optimization design. For the balanced exploration and exploitation, each objective function was converted to the expected improvements (EI) and this value was directly used as fitness values in the multi-objective optimization. As an optimizer, multi-objective genetic algorithm (MOGA) was

used here. From the non-dominated solutions about EIs, additional points for the update of the Kriging model were selected. The present method was applied to a transonic airfoil design. Design results showed the validity of the present method.

In order to obtain the information about design space, two data mining techniques were applied to design results: Analysis of Variance (ANOVA) and Self-Organizing Map (SOM). ANOVA shows the relation between objective functions and design variable quantitatively and SOM shows it qualitatively. For the intuitive understand of aerodynamic performance and the airfoil geometry, the design variables defined by NURBS was transformed into the geometry parameters which are more familiar to aerodynamic engineers. The results of data mining are consistent with the general aerodynamic knowledge. These indicate that ANOVA and SOM used in this study are valid for data mining of aerodynamic design space.

References

1. Myers, R. H. and Montgomery, D. C, Response Surface Methodology: Process and Produc t Optimization Using Designed Experiments, John Wiley & Sons, New York, 1995.

2. Vicini, A. and Quagliarella, Multipoint transonic airfoil design by means of a multiobjectiv e genetic algorithms, AIAA Paper 1997-82.

3. Sasaki, D., Obayashi, S and Nakahashi, K., Navier-Stokes Optimization of Supersonic Wi ngs with Four Objectives Using Evolutionary Algorithm, Journal of Aircraft, Vol. 39, 2003, pp621-629.

4. Jone, D. R., Schonlau, M. and Welch, W. J, Efficient Global Optimization of Expensive Bla ck-Box Function, Journal of global optimization, Vol. 13, 1998, pp. 455-492.

5. Jeong, S., Murayama, M. and Yamamoto, K., Efficient Optimization Design Method Using Kriging Model, Journal of Aircraft, Vol. 42, 2005, pp. 412-420.

6. Knowles, J. and Hughes, E. J., Multiobjective Optimization on a Budget of 250 Evaluation, Proceeding of third international conference of EMO 2005, 2005, pp. 176-190.

7. Sack, J., Welch, W. J., Mitchell, T. J. and Wynn, H. P., Design and analysis of computer experiments (with discussion), Statistical Science 4, 1989, pp. 409-435.

8. Matthias, S., Computer Experiments and Global Optimization, Ph.D Dissertation, Statistic and Actuarial Science Dept., University of Waterloo, Waterloo, Ontario, 1997.

9. Krzysztof, J. C., Witold, P. and Roman, W. S., Data Mining Methods for Knowledge Disco very, Kluwer Academic Publisher, 1998.

10. Eudaptics software gmbh, http://www.eudaptics.com/somine/index.php?sprache=en, last access on April 14, 2005.

11. Lepine, J., Guibault, F., Trepanier, J-Y., and Pepin, Optimized Nonuniform Rational B-spl ine Geometrical Representation for Aerodynamic Design of Wings, AIAA Journal, Vol. 39, 2001.

12. Mckay, M. D., Beckman, R. J. and Conover, W. J., A Comparison of Three Methods for Selecting Values of Input Variables in the Analysis of Output from a Computer Code, Technometr ic, Vol. 21, No. 2, 1979, pp. 239-245.